Neoplasia 67 (2025) 101195

Contents lists available at ScienceDirect

Neoplasia

journal homepage: www.elsevier.com/locate/neo

Original Research

Cancer-associated VEGFR2^{R1032Q} sustains receptor activation also by promoting ligand-independent hetero-dimerization with co-expressed wild-type VEGFR2 and translocation into lipid rafts

Cosetta Ravelli [a,b], Michela Corsini [a,b], Roberto Bresciani [a,b,c], Angela M. Rizzo [d], Luca Zammataro [e], Paola A. Corsetto [d], Elisabetta Grillo [a,b,1], Stefania Mitola [a,b,1,*]

[a] Department of Molecular and Translational Medicine, University of Brescia, Brescia, 25123, Italy
[b] The Mechanobiology Research Center, University of Brescia, Brescia, Italy
[c] Highly Specialized Laboratory, ASST Spedali Civili of Brescia, Brescia, 25123, Italy
[d] Department of Pharmacological and Biomolecular Sciences, University of Milan, Milano, 20133, Italy
[e] Lunan Foldomics LLC, Houston, TX, 77057, USA

ARTICLE INFO

Keywords:
VEGFR2
R1032Q mutant
Dimerization
Ligand-independent receptor hyperactivation
Membrane microdomains

ABSTRACT

The substitution R1032Q is the most frequent non-synonymous mutation of the vascular endothelial growth factor receptor 2 (VEGFR2) in cancer patients, classified as a loss-of-function variant. Here we characterize the molecular bases of its role in cancer, demonstrating that it lacks significant activity and pro-oncogenic effects in VEGFR2-negative tumor cells, while being able to sustain the tumorigenic potential of VEGFR2-positive cancer cells. By implementing a cell model that allows expression of either VEGFR2^{R1032Q} alone or in combination with VEGFR2^{WT}, we showed that the effects of mutated VEGFR2 are at least in part due to the ability of VEGFR2^{R1032Q} to form functional heterodimers with co-expressed VEGFR2^{WT} that result in increased kinase activity and receptor phosphorylation. This was associated with reduced mobility of the receptor on the membrane, linked to its translocation into detergent-resistant membrane (DRM) domains (e.g. lipid rafts), which showed alterations in lipid compositions and structure. These data shed light on a novel oncogenic mechanism of activation of VEGFR2, clarifying the paradoxical loss-of-function nature of the substitution R1032Q of VEGFR2.

Introduction

In recent years, the vascular endothelial growth factor receptor 2 (VEGFR2) has emerged as a central player of tumor progression, involved in controlling both stromal and parenchymal tumor compartments. VEGFR2 regulates the infiltration of immune cells, promotes angiogenesis and sustains cancer cell proliferation, invasion, metabolic rewiring and stemness [1–3]. On these bases, VEGFR2-targeted drugs, including tyrosine kinase inhibitors (TKi), that had been originally developed as anti-angiogenic drugs, are thought to exert multi-compartment effects, also directly hampering tumor cell proliferation and metastasization.

VEGFR2 is recurrently dysregulated in cancer cells. VEGFR2 dysregulation occurs *via* gene amplifications, rare structural variants, deletions and point mutations. Among all VEGFR2 point mutations, missense mutations are the most frequent ones. Increasing experimental and clinical evidence corroborates that VEGFR2 missense mutations alter tumor progression and response to therapeutics, including VEGFR2-targeted TKi [4–9]. However, the exact molecular mechanism by which those mutations alter receptor function and cancer progression remains scarcely explored, while it may hide novel mechanisms of activation of VEGFR2 with prognostic and/or therapeutic significance.

We recently demonstrated that R1051Q and D1052N substitutions of VEGFR2 make the receptor constitutively active (i.e. gain-of-function) [6]. On the other hand, a loss of function has been proposed for other mutations, including the most frequent alteration of VEGFR2 found in cancer patients, namely the R1032Q substitution [10]. A clear association between cancer progression and VEGFR2 "loss-of-function" variants exists, but the underlying mechanism has not been clarified yet.

RTKs that lack phosphotransferase activity play crucial roles in the

* Corresponding author at: Department of Molecular and Translational Medicine, University of Brescia, Via Branze 39, Brescia, 25123, Italy.
E-mail address: stefania.mitola@unibs.it (S. Mitola).
[1] Co-last authors.

https://doi.org/10.1016/j.neo.2025.101195
Received 8 April 2025; Received in revised form 2 June 2025; Accepted 5 June 2025
Available online 14 June 2025

regulation of RTK signaling. They can act as scaffolding proteins, forming complexes with functional RTKs and regulating (i.e. promoting or inhibiting) their dimerization, activation and signaling. Also, RTK activation is regulated by ligand interaction and dimerization and by the biophysical properties of lipidic membrane environment. Increasing evidence highlights the critical contribution of membrane lipids in modulating RTK activation, extending beyond their structural role to that of dynamic regulators of receptor organization and function [11–13]. In particular, lipid rafts are specialized and rigid membrane domains that modulate RTK dimerization and dynamics. Indeed, the recruitment in lipid rafts serves as an organizational scaffold for receptors and associated signaling molecules, supporting signaling amplification and protein recycling [14–16]. On these bases, it could be speculated that intrinsically inactive RTKs may affect the organization of membrane lipid domains through their interaction with the lipid bilayer regulating the membrane dynamics of co-expressed membrane proteins (e.g. active RTKs). These considerations are crucial for the characterization of the R1032Q mutation in cancer patients, particularly given that this alteration is detected in a heterozygous state (*source: cBioPortal*) where both wild-type and mutant VEGFR2 co-exist and may influence each other. To better elucidate these aspects, we performed a mechanistic analysis of the effects of the R1032Q substitution on receptor function. By comparing the effects of VEGFR2^{R1032Q} expression in VEGFR2 negative *vs* VEGFR2 positive cancer cells we demonstrated that it acquires pro-oncogenic activity in the presence of VEGFR2^{WT}, while retaining its loss-of-function nature in a VEGFR2^{-} background. We also implemented a cell model enabling the expression of VEGFR2^{R1032Q} alone or in combination with VEGFR2^{WT}. Using this system, we noticed that VEGFR2^{R1032Q} forms functional dimers with wild-type VEGFR leading to ligand-independent receptor activation and phosphorylation. This aberrant activation is associated with a reduced membrane mobility, redistribution into detergent-resistant membrane (DRM) microdomains, and alterations of the DRM lipid composition. Altogether our data clarify the role of the mutation R1032Q in cancer, suggesting ligand-independent mechanisms of activation of VEGFR2.

Material and methods

Mutagenesis

pBE_hVEGFR2 plasmid encoding for wild-type hVEGFR2 [NM_002253.2] and pBE_hVEGFR2^{K868M} were kindly provided by Prof. Kurt Ballmer-Hofer (Paul Scherrer Institut, PSI, Villigen, Switzerland). pBE_hVEGFR2-YFP, and pBE_hVEGFR2-mCherry were kindly provided by Dr. Kalina Hristova (Johns Hopkins University, Baltimore, Maryland, USA) [17]. pBE_hVEGFR2^{R1032Q} plasmid was generated using the QuikChange Lightning Site-directed Mutagenesis Kit (Agilent Technologies, California, USA). To introduce the R1032Q point mutation the following primers were used: forward 5′-GGGACCTGGCGG CACAAAATATCCTCTTATCG-3′ and reverse 5′-CGATAAGAGGATA TTTTGTGCCGCCAGGTCCC-3′. Similarly, pBE_hVEGFR2-YFP was mutagenized to generate pBE_hVEGFR2^{R1032Q}-YFP.

Cell cultures

Human breast adenocarcinoma cell line MCF7 (purchased from American Type Culture Collection - ATCC) was grown in DMEM supplemented with 10 % FCS (Invitrogen, Massachusetts, USA) and penicillin/streptomycin. Porcine aortic endothelial cells (PAECs) [18] were cultured in DMEM supplemented with 10 % FCS and penicillin/streptomycin. Human melanoma Sk-Mel-31 cells were provided by the Memorial Sloan Kettering Cancer Center (MTA MSK00005207). Sk-Mel-31 cells were grown in RPMI supplemented with 10 % FCS, non-essential amino acids and penicillin/streptomycin. Sk-Mel-31 cells were sequenced and found to express wild-type VEGFR2. MCF7 and Sk-Mel-31 cells stably expressing VEGFR2^{WT} or VEGFR2^{R1032Q} were generated by transfection of pBE_hVEGFR2 or pBE_hVEGFR2^{R1032Q} plasmids using FuGENE Transfection Reagent (Promega Corporation, Wisconsin, USA), followed by selection with 0.5 mg/mL geneticin. Two different transfections were performed and achieved similar VEGFR2 expression levels. All experiments were conducted with both cell populations. Transfected cell lines were maintained in 0.5 mg/mL geneticin. Chinese hamster ovary (CHO) cells were grown in Ham's F-12 supplemented with 10 % FCS and penicillin/streptomycin. CHO cells were transiently transfected with pBE_hVEGFR2 or pBE_hVEGFR2^{R1032Q} plasmids using polyethylenimine (PEI) transfection reagent (Polysciences, Inc, Warrington, USA). Each experiment was repeated using at least three different transfections. Cells were grown at 37°C, under a humidified atmosphere, with 5 % CO_2. Cells were checked monthly for mycoplasma contamination.

Immunoprecipitation and Western-blot analyses

Cells were lysed in lysis buffer [50 mM Tris-HCl buffer (pH 7.4), 150 mM NaCl, 1 % Triton X-100, 1 mM Na_3VO_4, and protease inhibitors (Merck Sigma, Germany)]. When indicated cells were stimulated for 10 minutes at 37°C with 30 ng/mL of recombinant VEGF-A (R&D Systems, Minnesota, USA). Next, total lysates were separated by SDS-PAGE and probed with anti-VEGFR2 (clone D5B1, 9698S, Cell signaling Technology, Massachusetts, USA), anti-phospho-VEGFR2 (Tyr 1175) (MA5-15170, Thermo Fisher Scientific, Massachusetts, USA), anti-FAK (AHO0502, Thermo Fisher Scientific), anti-Grb2 (Santa Cruz Biotechnology, Texas, USA), anti-Shp2 (Santa Cruz Biotechnology) or anti-Nck (Santa Cruz Biotechnology) antibodies in a Western blot (WB). Alternatively, lysates were analyzed using a human phospho-receptor tyrosine kinase array kit (R&D Systems) following manufacturer's instructions. To verify the purity of isolated DRMs and DSMs (see below), membrane fractions were separated by SDS-PAGE and probed with anti-flotillin 1 (sc-25506, Santa Cruz Biotechnology) antibody. For immunoprecipitation, 1 mg of total lysate was immunoprecipitated with anti-total-phospho-tyrosine antibody (clone 4G10, 05-321 EMD Millipore Corp. Massachusetts, USA) or anti-VEGFR2 (sc-6251 Santa Cruz Biotechnology) and probed with anti-VEGFR2 antibody (clone D5B1, 9698S, Cell Signaling Technology, Massachusetts, USA). Chemiluminescent signal was acquired by ChemiDoc^{TM} Imaging System (BioRad, California, USA) and analysed with ImageLab software from BioRad.

2D and 3D proliferation and clonogenic assays

12 × 10^3 non-transfected MCF7 cells or VEGFR2^{WT} or VEGFR2^{R1032Q}-expressing MCF7 cells were seeded in a 48 well plate in DMEM/F12 2 % FCS and their growth was monitored after 72 hours. For 3D cell growth, 48 well plates were coated with 100 µl of Cultrex (15.51 mg/mL Cultrex BME, Biotechne, Minnesota, USA). 12 × 10^3 non-transfected MCF7 cells or expressing VEGFR2^{WT} or VEGFR2^{R1032Q} were seeded into Cultrex-coated wells in DMEM/F12 medium added with 2 % FCS and 4 % Cultrex. Cells were grown at 37°C for 4 days to allow MCF7 to grow and organize in spheroids. Spheroids were observed under an inverted microscope (Zeiss Axiovert 200 M, Carl Zeiss, Germany) and phase contrast snap photographs were digitally recorded. Spheroid areas were measured with ImageJ software.

For 2D clonogenic assays, non-transfected Sk-Mel-31 cells or expressing VEGFR2^{WT} or VEGFR2^{R1032Q} were seeded at a density of 1 × 10^2 cells/cm^2 and cultured in growth medium until visible colonies were formed. Next, cells were fixed and stained with 0.1 % crystal violet/20 % methanol and photographed. Cell growth area was measured by ImageJ analysis software. For the 3D clonogenic assay, Sk-Mel-31 cells were embedded at low density in soft agar gel. After 15 days cell colonies were photographed, and the colony area was calculated by ImageJ analysis software.

FLIM/FRET analysis

To perform fluorescence lifetime imaging microscopy (FLIM), we used pBE_hVEGFR2-YFP or pBE_hVEGFR2^{R1032Q}-YFP as FRET donors and pBE_hVEGFR2-mCherry as FRET acceptor. CHO cells were transiently transfected with donor plasmid alone (for donor only control) or co-transfected with both donor and acceptor plasmids (at DNA ratio of 1:1). The fluorescence lifetime of donor fluorophore without or with the acceptor fluorophore was evaluated with a two-photon LSM880 laser-scanning microscope equipped with a time-correlated single-photon counting (TCSPC) module (PicoQuant, Germany). The donor was excited at 860 nm using a picosecond pulsed with a Chameleon Vision II laser at a 80 MHz repetition rate (Coherent Inc, California, USA). The TCSPC decay curves were fitted using the SymphoTime 64 software (PicoQuant). For each individual cell, the YFP-positive cell membrane was selected as the region of interest, and the average lifetime within the region of interest was determined. YFP has a mono-exponential decay and in our experiment it showed a lifetime of approximately 2.3 ns, consistent with previous reports [19,20]. In the presence of the mCherry-tagged acceptor, we analyzed the data using a bi-exponential decay fitting model. FRET efficiency was calculated using amplitude-weighted average lifetimes (τ) which accurately reflect donor quenching due to FRET. The FRET efficiency (E) was then calculated using the standard equation: $E = 1-(\tau DA/\tau D)$ where τ_D is the donor lifetime in the absence of the acceptor, and τ_DA is the average donor lifetime in the presence of the acceptor.

VEGFR2 kinase and phosphorylation assays

Total lysates (1-2 mg) of CHO cells expressing untagged or YFP-tagged VEGFR2^{R1032Q} or VEGFR2^{WT} were immunoprecipitated with limiting amounts of anti-VEGFR2 antibody (sc-6251, Santa Cruz Biotechnology) or with anti-GFP antibody (Abcam, UK) using ProteinA-Sepharose beads (Cytiva, Massachusetts, USA). Where indicated, VEGFR2-containing immunocomplexes absorbed onto ProteinA-Sepharose (PtA) were incubated with 200 μg of whole lysate of VEGFR2^{R1032Q}- or VEGFR2^{WT}-CHO cells, 100 mM ATP and 25 mM $MgCl_2$ (kinase reaction buffer) for 45 minutes at 22°C. The kinase activity of VEGFR2 adsorbed onto PtA was analyzed using ADP-Glo Kinase Assay + KDR Kinase Enzyme System (Promega Corporation, Wisconsin, USA). Briefly, VEGFR2 adsorbed onto PtA was incubated for 1 hour at room temperature with poly (4:1 Glu, Tyr) peptide substrate and 50 μM ATP in specific buffer. Then, ADP-glo assay was performed according to the manufacturer's instructions. Bioluminescent signal was measured with the EnSight Multimode Plate Reader (PerkinElmer, Massachusetts, USA). Alternatively, after incubation with lysates in kinase buffer, GFP-immunocomplexes were analyzed by SDS-PAGE followed by anti-total-phospho-tyrosine (clone 4G10, 05-321 EMD Millipore) Western blot.

Analysis of membrane receptor dynamics by fluorescence recovery after photobleaching (FRAP)

Transfected cells were seeded at 5.0×10^5 cells/mL in μ-slides (ibidi) and analyzed using LSM880 confocal microscope equipped with an incubation chamber (Carl Zeiss). When indicated cells were treated with 30 ng/mL of recombinant VEGF-A. Images were recorded with 2 % of the intensity of the 514-nm line. YFP was bleached using 100-iteration at 100 % intensity of the 514-nm line in 2-3 regions of interest (ROIs)/cell smaller than 2 % of the total cell area (~1 μm^2) in the ring-like membrane area and leading to 80 % reduction of YFP intensity. ROIs for the analysis were selected specifically on cell membrane. Fluorescence recovery in bleached areas was followed for 4 minutes (1 image/0.5 min) and analyzed using the FRAP tool of Zen black software (Carl Zeiss). Data were corrected for back-ground and incidental bleaching measured in independent ROIs. Then data were fitted using the follow formula: I=IE-I1*exp(-t/T1). Diffusion Rate=1/thalf, were thalf is equal to (ln0.5)*T1. The mobile fraction was instead determined by comparing the fluorescence in the bleached region after full recovery (F∞) with the fluorescence before bleaching (Fi) and just after bleaching (F0). The mobile fraction R was defined as: R= (F∞- F0)/(Fi- F0) [20,21].

Detergent-resistant membranes isolation and lipid analysis

CHO cells expressing VEGFR2^{WT}, both unstimulated and treated with 30 ng/mL of VEGF for 10 minutes at 37°C, cells expressing VEGFR2^{R1032Q}, and cells co-expressing VEGFR2^{WT} and VEGFR2^{R1032Q} were harvested by scraping, washed with cold PBS and 0.4 mM Na_3VO_4 and centrifuged at 1300 g for 5 minutes at 4°C. Samples were lysed using TNE-lysis buffer containing 1 % Triton X-100 and a complete protease inhibition cocktail. The lipid rafts were isolated as detergent resistant membranes (DRMs) on a sucrose density gradient as already described [22] and, after ultracentrifugation, 11 fractions were collected.

For lipid analysis, 700 μL of each fraction was extracted by Folch method with minor modifications. Total fatty acids (FAs) (saturated, mono- and polyunsaturated) were determined as methyl esters (FAME) using a Shimadzu (GC-2025, Japan) gas chromatograph equipped with a flame ionization detector. A standard mixture containing all FAME was injected for calibration, and TG C17:0 was added before sample manipulation and used as internal standard. Sphingomyelin (SM) and cholesterol (Chol) were quantified by HPLC system (Jasco, Japan) equipped with an Sedex LT-ELSD detector (model 80LT, LTSedere, France) and silica normal-phase LiChrospher Si 60 column (LiChroCART 250-4; Merck, Germany).

In vivo tumorigenesis

In vivo experiments approved by Italian "Ministero della Salute" (authorization 266/2016-PR) were performed in accordance with national and European guidelines and regulations. Mice were obtained from Envigo (Italy) and housed at the Mouse Facility of the Department of Molecular and Translational Medicine of the University of Brescia. Mice were housed in ventilated cage racks at 22-24°C, under a 12 h:12 h light/dark cycle and with *ad libitum* access to food and water. NOD/Scid mice were injected subcutaneously (s.c.) into the dorsolateral flank with 100 μl (1:1 PBS:Cultrex) containing 4×10^6 Sk-Mel-31-VEGFR2^{WT} or Sk-Mel-31-VEGFR2^{R1032Q} cells. Tumor growth was followed over time and tumor volume was measured with calipers and calculated according to the formula V=(Dxd [2])/2, where D and d are the major and minor perpendicular tumor diameters, respectively.

Immunofluorescence

Formalin-fixed paraffin-embedded (FFPE) tissue sections were stained with anti-pVEGFR2 antibody (Tyr 951; sc-16628-R, Santa Cruz Biotechnology). Antigen retrieval was performed in EDTA buffer solution (0.05 M and pH 8.0) at 95°C for 20 minutes before immunostaining. Nuclei were counterstained with TO-PRO-3 iodide (T3605, Molecular Probes, Oregon, USA). Images were captured using Axio Observer (Carl Zeiss) equipped Apotome.2 and with Plan-Apochromatic 63X/1,4 Oil DIC objective and analyzed by Zen software (Carl Zeiss).

Statistical analyses

Student's *t*-test for unpaired data (2-tailed) was used to test the probability of significant differences between two groups of samples. One-Way ANOVA followed by Dunnett's post-hoc test was used for multiple comparisons. Differences were considered significant when $p < 0.05$. *, $p < 0.05$; **, $p < 0.01$; ***, $p < 0.001$ and ****, $p < 0.0001$. Error bars in graphs represent the standard error of the mean (SEM).

Results

The VEGFR2^{R1032Q} exhibits a transition from loss-of-function to gain-of-function effects in VEGFR2 negative vs VEGFR2 positive cells, enhancing the tumorigenic ability of melanoma cells

A pan-cancer analysis of gene alterations shows that VEGFR2 is recurrently mutated with a somatic mutation frequency of 2.3 %. The somatic missense mutation R1032Q is the most frequently observed variant (*source: curated set of non-redundant studies as suggested by cBioPortal,* https://www.cbioportal.org*, February 2025*). Although previously characterized as a loss of function mutation [10], VEGFR2^{R1032Q} paradoxically triggers tumor growth when expressed in a murine model of colon cancer [5]. To further investigate its pro-oncogenic effects and clarify this paradox, we examined the impact of VEGFR2^{R1032Q} expression in VEGFR2^{-} *vs* VEGFR2^{+} cell models. Thus, VEGFR2^{R1032Q} was expressed in MCF7 breast cancer cells that express non-detectable levels of endogenous VEGFR2 and in Sk-Mel-31 melanoma cells bearing basal levels of endogenous wild-type VEGFR2. Isogenic cell lines transfected with VEGFR2^{WT} were used as controls (Fig. 1a).

In both cell lines, the expression of VEGFR2^{WT} enhanced 2D cell proliferation (Fig 1b and c). VEGFR2^{R1032Q} expression had negligible effects on the 2D *in vitro* proliferation of MCF7 cells, while it significantly increased the 2D *in vitro* proliferation of VEGFR2-positive Sk-Mel-31 cells (Fig. 1b and c) and endothelial cells (Fig. SI). In 3D assays, the expression of VEGFR2^{R1032Q} exerted an inhibitory effect on the proliferation of MCF7 cells compared to VEGFR2^{WT}. On the contrary, it strongly increased the growth of Sk-Mel-31 cells (Fig. 1d and e).

The effects of VEGFR2^{R1032Q} in VEGFR2-negative MCF7 cells are in line with the previously reported loss-of-function nature of the R1032Q substitution in VEGFR2. On the other hand, although further confirmation on isogenic lines is necessary, the pro-proliferative impact of the expression of VEGFR2^{R1032Q} in VEGFR2-positive Sk-Mel-31 melanoma cells support the hypothesis that mutated VEGFR2^{R1032Q} could promote tumor growth when co-expressed with wild-type VEGFR2. Consistent with this hypothesis, Sk-Mel-31-VEGFR2^{R1032Q} cells demonstrated enhanced tumorigenic capacity in a *in vivo* xenograft model (Fig. 1f). Immunofluorescence analyses revealed higher VEGFR2 phosphorylation in Sk-Mel-31-VEGFR2^{R1032Q}-derived tumors (Fig. 1g) compared to control tumors.

VEGFR2^{R1032Q}/VEGFR2^{WT} heterodimerization sustains receptor activity and phosphorylation

As anticipated, the enhanced growth of Sk-Mel-31-VEGFR2^{R1032Q}-derived tumors prompted us to investigate whether VEGFR2^{R1032Q} could interact and affect co-expressed VEGFR2^{WT}, potentially explaining the increased receptor phosphorylation observed in Sk-Mel-31-VEGFR2^{R1032Q}-derived tumors. In order to verify this hypothesis, we established a CHO cellular model expressing VEGFR2^{WT} and VEGFR2^{R1032Q} alone or in combination with VEGFR2^{WT}. The expression of untagged-, YFP-tagged- and mCherry-tagged-VEGFR2 variants allowed us to specifically monitor the receptor variants.

In this model, when expressed singularly, VEGFR2^{WT} exhibited a basal phosphorylation, whereas VEGFR2^{R1032Q} was completely devoid of phosphorylation at Tyr^{1175} (Fig. 2a) both in the absence or the presence of VEGF stimulation, confirming previous observations [10]. Moreover, VEGFR2^{R1032Q} resulted in the loss of receptor phosphorylation at any tyrosine residue, as demonstrated by the lack of total phospho-tyrosine signal in VEGFR2-immunocomplexes (Fig. 2b). In contrast, CHO cells which co-express YFP-tagged VEGFR2^{WT} and untagged VEGFR2^{R1032Q} exhibited a significantly increased Tyr^{1175} VEGFR2 phosphorylation compared to cells expressing either the YFP-VEGFR2^{WT}/VEGFR2^{WT} couple or YFP-VEGFR2^{WT} alone. Of note, the co-expression resulted in the phosphorylation of both untagged VEGFR2^{R1032Q} (lower molecular weight) and YFP-VEGFR2^{WT} (higher molecular weight), as demonstrated by WB analyses (Fig. 2c). This data demonstrated that, despite being a loss-of-function mutation, VEGFR2^{R1032Q} remained competent for phosphorylation and able to boost VEGFR2 activation when in the presence of VEGFR2^{WT}. The substitution R1032Q favored receptor dimerization with VEGFR2^{WT}, as evidenced by increased FRET efficiency between YFP-VEGFR2^{R1032Q} and mCherry-VEGFR2^{WT} compared to the YFP-VEGFR2^{WT}/mCherry--VEGFR2^{WT} pair, measured by FLIM/FRET experiments (Fig. 2d). This enhanced interaction occurred in the absence of exogenous ligands and was similar to the VEGF-induced dimerization of wild-type VEGFR2 couple.

Previous findings showed that VEGFR2^{R1032Q} alone lacks significant kinase activity [10]. To evaluate whether VEGFR2^{R1032Q} can acquire enzymatic activity upon dimerization with VEGFR2^{WT}, the kinase activity of proteinA Sepharose (PtA)-adsorbed VEGFR2^{WT} or VEGFR2^{R1032Q} immunocomplexes was measured before and after incubation with total lysates of VEGFR2^{WT}- or VEGFR2^{R1032Q}-expressing CHO cells. This incubation was performed to activate the adsorbed receptor by temporary receptor interaction. While the enzymatic activity of PtA-absorbed-VEGFR2^{WT} remained unchanged upon both incubation with VEGFR2^{WT} or VEGFR2^{R1032Q} lysates, the kinase activity of PtA-adsorbed VEGFR2^{R1032Q}-immunocomplexes increased significantly upon incubation with VEGFR2^{WT}-expressing CHO lysate (Fig. 2e). Also, the phosphorylation levels of PtA-adsorbed YFP-VEGFR2^{WT} or YFP--VEGFR2^{R1032Q} were analysed before and after incubation with total lysates of VEGFR2^{WT}- or VEGFR2^{R1032Q}-expressing CHO cells. After 45 minutes of incubation, the phosphorylation of PtA-adsorbed YFP--VEGFR2^{WT} or YFP-VEGFR2^{R1032Q} alone or incubated with the matching lysates were low-to undetectable. In contrast, the reciprocal co-incubation of VEGFR2^{WT} and VEGFR2^{R1032Q} led to significant receptor phosphorylation. These findings suggested that the mutant receptor can acquire kinase activity and that the co-expression of the two forms promotes reciprocal phosphorylation, occurring possibly upon receptor heterodimerization.

To characterize the recruitment of VEGFR2-associated intracellular signaling molecules, VEGFR2 immunocomplexes were analyzed for the presence of Shp2 phosphatase and Grb2 and Nck adaptor molecules. The amount of co-precipitated Shp2 strongly decreases when the heterocouple is expressed, compared to cells expressing only VEGFR2^{WT}. Similarly, the co-expression leads to a decrease in co-precipitated Grb2 and Nck, pointing to a different signaling activity of the VEGFR2^{WT}/VEGFR2^{R1032Q} heterodimers (Fig. 3). This abnormal activation of the VEGFR2 is paralleled by the activation of several RTKs, including VEGFR1 and VEGFR3, in Sk-Mel-31-VEGFR2^{R1032Q} (Fig. SII). Altogether, these data indicate that VEGFR2^{R1032Q}, when co-expressed with VEGFR2^{WT}, can acquire tumorigenic activity, at least in part, by promoting dimerization with the wild-type receptor, leading to enhanced receptor kinase activity, phosphorylation and altered signaling.

VEGFR2^{R1032Q} alters the mobility and localization of VEGFR2 within membrane microdomains and modifies the membrane lipid composition

We previously demonstrated that membrane dynamics and VEGFR2 activity are interdependent [6,20]. To deepen the bases of the increased activity of VEGFR2^{R1032Q}/VEGFR2^{WT} heterodimers, we investigated the lateral membrane mobility of YFP-VEGFR2^{WT} and YFP-VEGFR2^{R1032Q} alone or co-expressed with VEGFR2^{WT} and/or VEGFR2^{R1032Q}. CHO cells were transfected with YFP-VEGFR2^{WT} or YFP-VEGFR2^{R1032Q} and receptor membrane displacement was measured by fluorescence recovery after photobleaching (FRAP) analyses. YFP-VEGFR2^{WT} exhibited a lateral diffusion rate of 0.020 while YFP-VEGFR2^{R1032Q} alone displayed a significantly slower diffusion rate. A similar reduction in lateral mobility was observed for YFP-VEGFR2^{WT} following VEGF stimulation. The co-expression of untagged VEGFR2^{R1032Q} did not affect the diffusion of YFP-VEGFR2^{WT}, and untagged VEGFR2^{WT} did not significantly modify the already low lateral mobility of YFP-VEGFR2^{R1032Q} (Fig. 4a

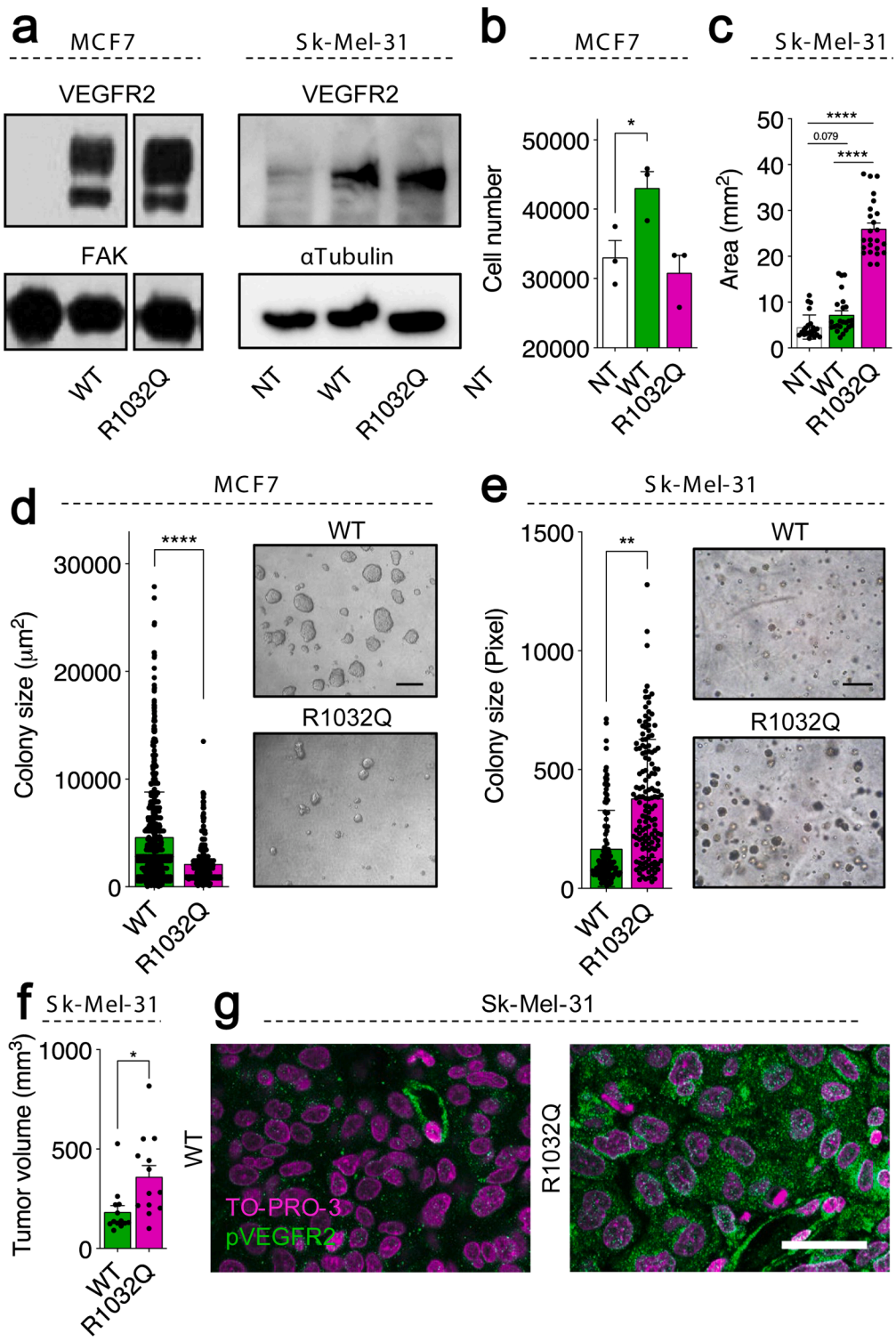

Fig. 1. Proliferative effects of VEGFR2^{R1032Q} expression in VEGFR2 negative vs VEGFR2 expressing cell models. **a**, Western blot (WB) analysis of total VEGFR2 levels in MCF7 or Sk-Mel-31 cells. Total lysates of non-transfected (NT) cells and of cells transfected to express VEGFR2^{WT} (WT) or VEGFR2^{R1032Q} (R1032Q) were analyzed. FAK and α-tubulin levels were measured as loading controls. Images are representative of three independent experiments that gave superimposable results. **b**, 2D MCF7 cell proliferation. Mean cell number of three biological replicates. **c**, 2D Sk-Mel-31 cell proliferation. Mean covered area ± SEM of $N = 24$ biological replicates from three independent experiments. *, $p < 0.05$, ****, $p < 0.001$, One-Way ANOVA followed by Dunnett's post-hoc test. **d**, 3D anchorage-independent MCF7 cell proliferation. Average size of N = 300-1200 cell aggregates from two independent experiments. Representative images, scale bar 200 μm. **e**, 3D anchorage-independent Sk-Mel-31 cell proliferation. Average size of N = 114-142 cell colonies from two independent experiments. Representative microphotographs, scale bar 200 μm. **f-g**, in vivo growth of Sk-Mel-31-VEGFR2^{WT} and Sk-Mel-31-VEGFR2^{R1032Q} cells injected subcutaneously into the flank of NOD/SCID mice (N = 11-12). Tumor volume after 35 days (**f**). Immunofluorescence analysis of pVEGFR2 (in green) in tumor FFPE sections at day 35 after implantation. TO-PRO-3 nuclei counterstaining is shown in magenta. Scale bar, 20 μm (**g**). *, $p < 0.05$, **, $p < 0.01$,***, $p < 0.005$, ****, $p < 0.001$, Student's t-test.

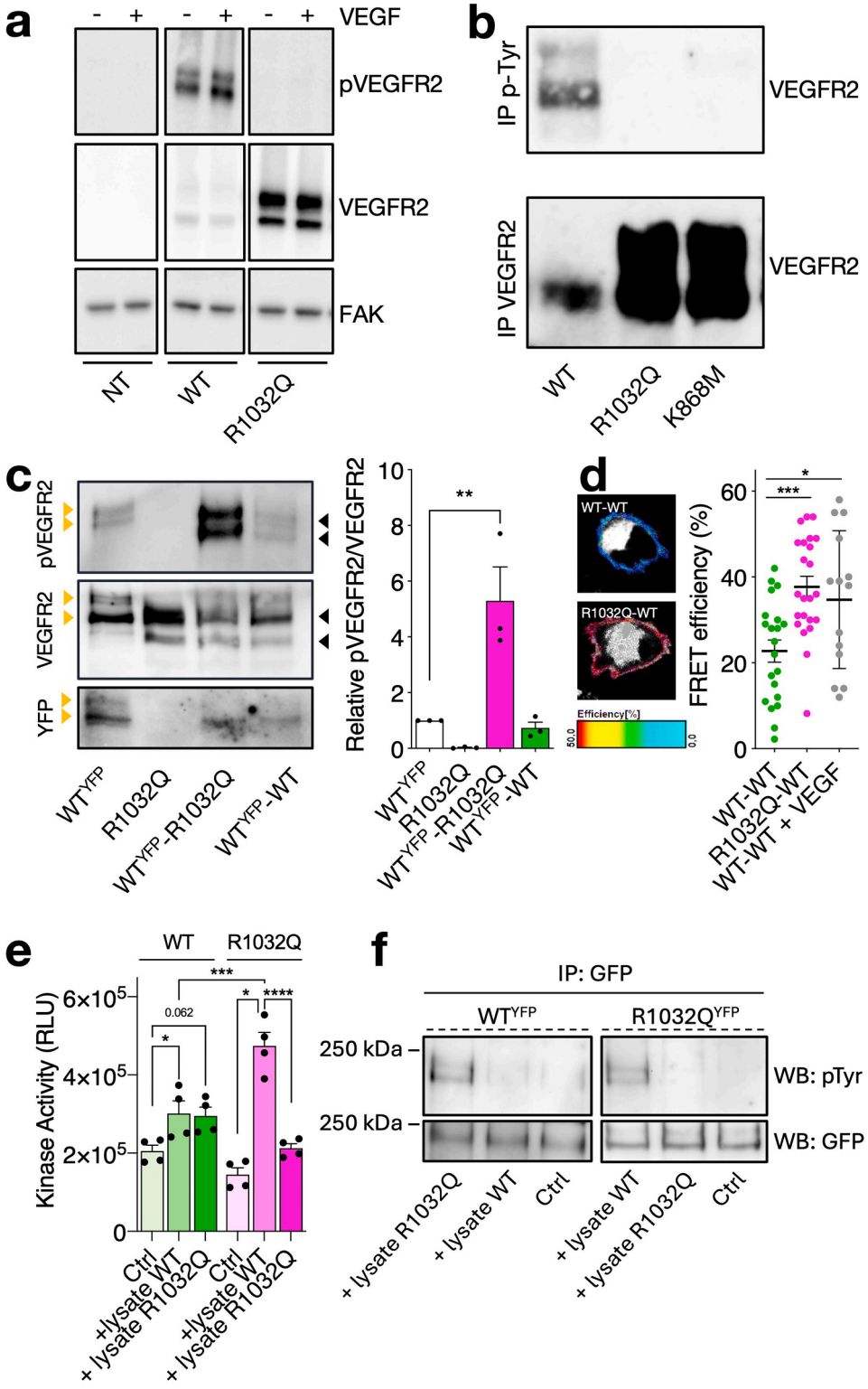

(caption on next page)

Fig. 2. VEGFR2^{R1032Q} forms functional heterodimers with co-expressed VEGFR2^{WT}. **a**, WB analysis of pVEGFR2 (Y1175) and total VEGFR2 levels in total lysates of serum-starved CHO cells (NT) or expressing VEGFR2^{WT} (WT) or VEGFR2^{R1032Q} (R1032Q) in the absence or in the presence of 30 ng/mL VEGF. FAK levels were measured as loading control. **b**, WB analysis using anti-VEGFR2 of total p-Tyr- (up) and Anti-VEGFR2 immunocomplexes (IP) (down) of serum-starved CHO cells expressing VEGFR2^{WT} or VEGFR2^{R1032Q} or the kinase-dead mutant VEGFR2^{K868M} (K868M) using antibodies anti VEGFR2. WB images are representative of three independent experiments that gave superimposable results. **c**, WB analysis of phospho-VEGFR2 (Tyr1175), VEGFR2 and YFP in total lysates of serum-starved CHO cells expressing YFP-tagged VEGFR2^{WT} alone or in combination with untagged VEGFR2^{WT} or VEGFR2^{R1032Q} or untagged VEGFR2^{R1032Q} alone. Yellow arrowheads, YFP-tagged VEGFR2. Black arrowheads, untagged VEGFR2. The densitometric quantification of 3 independent experiments is shown in the bar graph. **d**, FRET efficiency of mCherry-VEGFR2^{WT}-YFP-VEGFR2^{WT} or mCherry-VEGFR2^{WT}-YFP-VEGFR2^{R1032Q} couples expressed in CHO cells measured by FLIM. Representative color-coded FRET efficiency images of cell membrane ROI. FRET efficiency of the mCherry-VEGFR2^{WT}-YFP-VEGFR2^{WT} couple treated with VEGF was used as control. **e**, measurement of the kinase activity of PtA-adsorbed VEGFR2-immunocomplexes isolated from CHO cells expressing VEGFR2^{WT} or VEGFR2^{R1032Q} before (Ctrl) or after the incubation with the total lysate of CHO cells expressing VEGFR2^{WT} or VEGFR2^{R1032Q} to induce receptor dimerization. **f**, phosphorylation levels of PtA-adsorbed GFP-immunocomplexes isolated from CHO cells expressing VEGFR2$^{WT(YFP)}$ or VEGFR2$^{R1032Q(YFP)}$ before (Ctrl) or after the incubation with the total lysate of CHO cells expressing VEGFR2^{WT} or VEGFR2^{R1032Q} to induce receptor dimerization. *, $p < 0.05$; **, $p < 0.01$; ***, $p < 0.005$, One-Way ANOVA followed by Dunnett's post-hoc test.

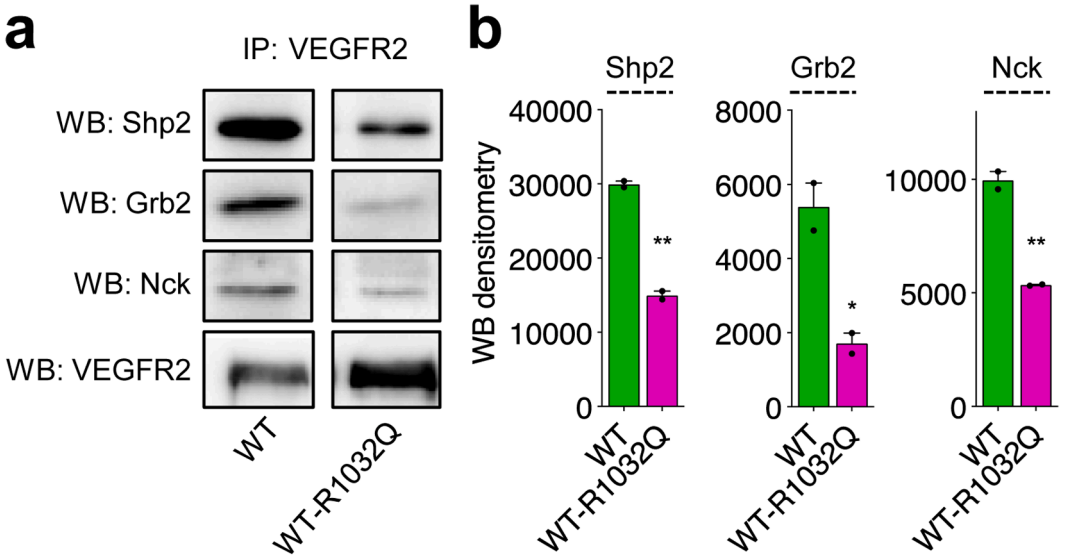

Fig. 3. Co-expression of VEGFR2^{WT}-VEGFR2^{R1032Q} alters the recruitment of intracellular signaling molecules. Total lysates of CHO cells transiently transfected with VEGFR2^{WT} or with VEGFR2^{WT} + VEGFR2^{R1032Q} were used to immunoprecipitate VEGFR2. **a**,immunoprecipitated fractions were analyzed by WB for the presence of Shp2, Nck and Grb2. Non-adjacent lanes of the same blot. **b**, WB densitometry and statistical analysis of 2 independent experiments was performed. *, $p < 0.05$; **, $p < 0.01$; Student's t Test *vs* VEGFR2^{WT}.

and SIII). In parallel, the fraction of immobile YFP-VEGFR2^{R1032Q} was significantly higher compared to YFP-VEGFR2^{WT} and similar to the one of VEGF-stimulated YFP-VEGFR2^{WT}. Also, the co-expression of untagged VEGFR2^{WT} reduced the immobile fraction of YFP-VEGFR2^{R1032Q}, while the co-expression of untagged VEGFR2^{R1032Q} did not affect the already low immobile fraction of YFP-VEGFR2^{WT} (Fig. 4b). To exclude possible effects due to different VEGFR2 expression levels, we compared FRAP results of cells with low *vs* high expression and found that both groups (low *vs* high) display a similar trend across the conditions and are consistent with the overall analysis (Fig. SIII).

The changes in receptor membrane mobility led us to hypothesize that VEGFR2^{R1032Q} and the hetero-dimer may exhibit altered distribution at specific membrane microdomains compared to the wild-type receptor alone. Thus, we next verified the localization of the VEGFR2^{WT}/VEGFR2^{R1032Q} complex in membrane microdomains. Detergent-resistant and detergent-soluble membrane (DRM and DSM respectively) fractions were isolated on a sucrose-density gradient. The DRM fractions (#5 and #6), confirmed by the presence of the lipid raft marker flotillin-1 (Flot1), were not significantly affected neither by the expression of VEGFR2 variants, nor by VEGF administration (Fig. 4). WB analyses revealed that the majority of VEGFR2, regardless of mutation status, was localized in DSM fraction #11 together with the early endosome marker EEA1. In basal conditions, VEGFR2^{WT} was homogenously distributed across DRM and DSM fractions (#5-#10) while VEGF stimulation induced its redistribution towards DSMs (#7-#10), in line with a previous report [23]. Similarly, inactive VEGFR2^{R1032Q} alone mainly localized in DSMs (#9-#10). In contrast, co-expression of VEGFR2^{WT} with VEGFR2^{R1032Q} resulted in a marked re-localization of total VEGFR2 towards DRMs (#5-#6). This data further confirm that a productive interaction between VEGFR2^{WT} and VEGFR2^{R1032Q} occurs and drives receptor translocation into lipid rafts.

To get insights into the activation mechanism of VEGFR2 heterodimeric complex, we assessed the localization of phosphorylated VEGFR2 in DRM *vs* DSM fractions by WB. As expected, VEGFR2^{R1032Q} alone remained unphosphorylated. Surprisingly, basally phosphorylated VEGFR2^{WT} was predominantly detected in fraction #10, while VEGF stimulation and the co-expression of VEGFR2^{WT} and VEGFR2^{R1032Q} promoted a shift of pVEGFR2 towards the early endosome compartments (fraction #11), compatible with its rapid internalization following activation (Fig. 5).

Since the lipid environment and the membrane stability of the receptor are very closely related we next analyzed the lipid composition of the membrane fractions as well as of total extracts of these CHO cells. The membrane lipid rafts, just like DRMs, are rich in saturated phospholipids, cholesterol (Chol) and sphingolipids, especially sphingomyelin (SM), compared to DSMs.

Lipidomic analysis of total extracts revealed no significant changes following expression of VEGFR2^{R1032Q} alone or in combination with VEGFR2^{WT} (Fig. 6a). The DRMs of CHO cells expressing VEGFR2^{R1032Q} displayed a membrane lipid composition similar to that of VEGFR2^{WT}

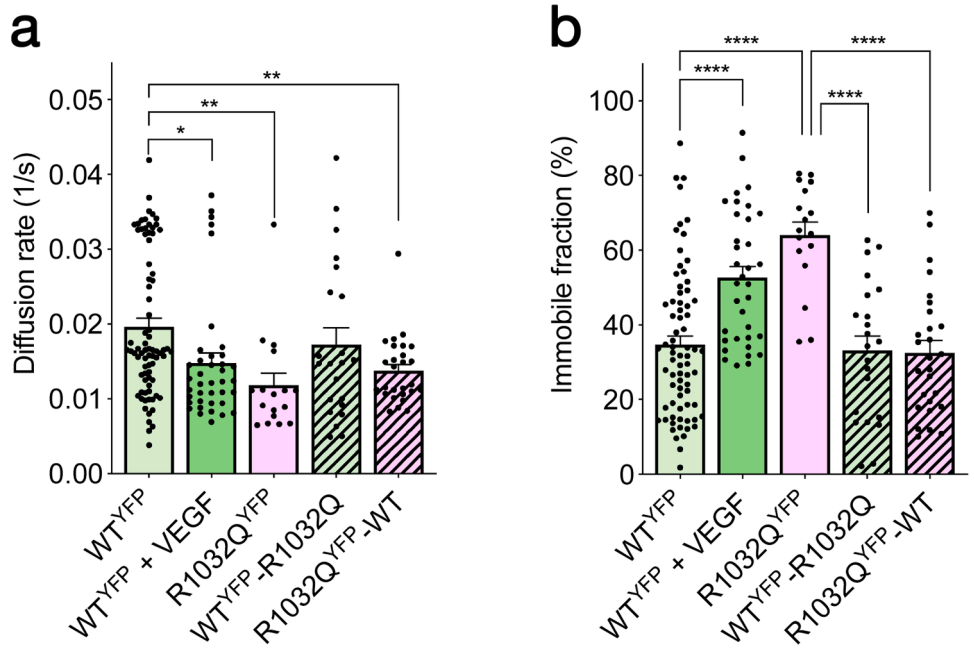

Fig. 4. The heterodimeric VEGFR2^{WT}-VEGFR2^{R1032Q} complex displays altered lateral membrane mobility. Diffusion rate (**a**) and immobile fraction (**b**) of YFP-tagged VEGFR2 variants (WT^{YFP} or R1032Q^{YFP}) alone or upon co-expression with untagged VEGFR2 variants as measured by FRAP analyses on the cell surface of transfected CHO cells. Stimulation with 30 ng/mL of VEGF of CHO cells expressing YFP-VEGFR2^{WT} was used as control. Data are shown as mean ± SEM of 2 independent experiments. Individual values of each replicate are shown. *, $p < 0.05$, ***, $p < 0.005$, One-Way ANOVA followed by Dunnett's post-hoc test.

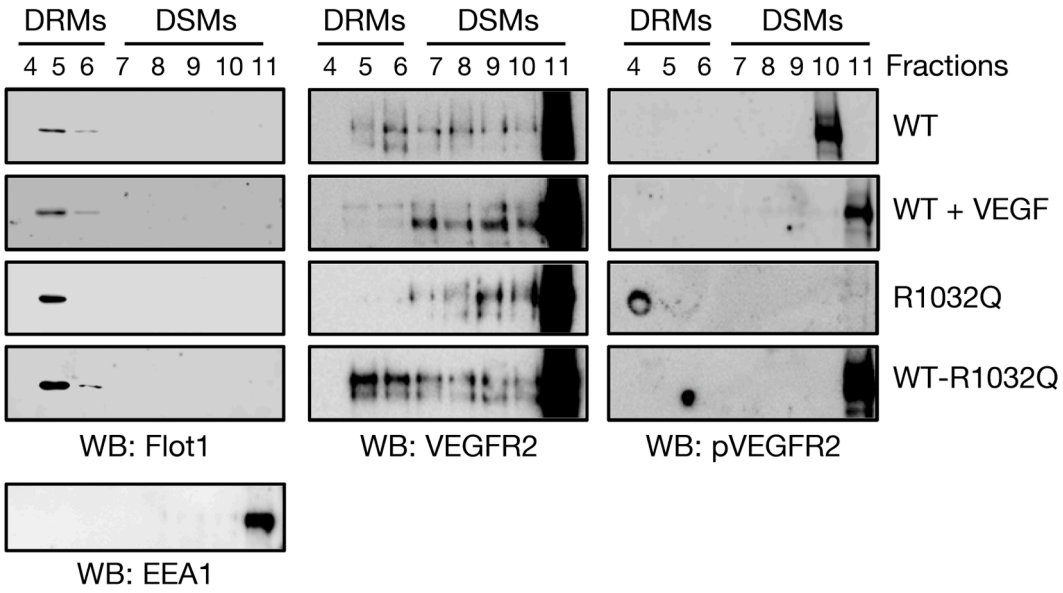

Fig. 5. VEGFR2 distribution within membrane microdomains. Western blot analysis of the levels of flotillin 1 (Flot1), early endosome antigen 1 (EEA1), total VEGFR2, and phospho-VEGFR2 (Tyr 1175) in DRM vs DSM membrane fractions of CHO cells expressing VEGFR2^{WT}, VEGFR2^{R1032Q} or the couple VEGFR^{WT}-VEGFR2^{R1032Q}. CHO- VEGFR2^{WT} was treated with 30 ng/mL of VEGF.

expressing cells. However, in cells co-expressing VEGFR2^{R1032Q}/VEGFR2^{WT}, we detected modest non-significant decreases of SFA, SM and cholesterol in DRM-associated lipids compared to cells expressing VEGFR2^{WT} alone. These alterations mirrored the membrane lipid changes induced by short-term (10 minutes) VEGF stimulation of VEGFR2^{WT} (Fig. 6b). The reduction in lipid raft-associated lipids upon VEGFR2^{R1032Q}/VEGFR2^{WT} co-expression may sustain receptor signaling in a ligand-independent manner, thereby supporting cancer growth.

Discussion

The R1032Q mutation is the most frequent alteration of VEGFR2 in cancer. Here we clarified the paradoxically cancer-promoting function of this inactivating mutation, providing new insights into how VEGFR2 operates in cancer.

The 1032 arginine residue of VEGFR2 corresponds to the second conserved arginine of the catalytic loop of the tyrosine kinase domain (HRDLAA**R**N). This arginine forms a hydrogen-bond with the sidechain of the aspartic acid that is important for the activation of the kinase

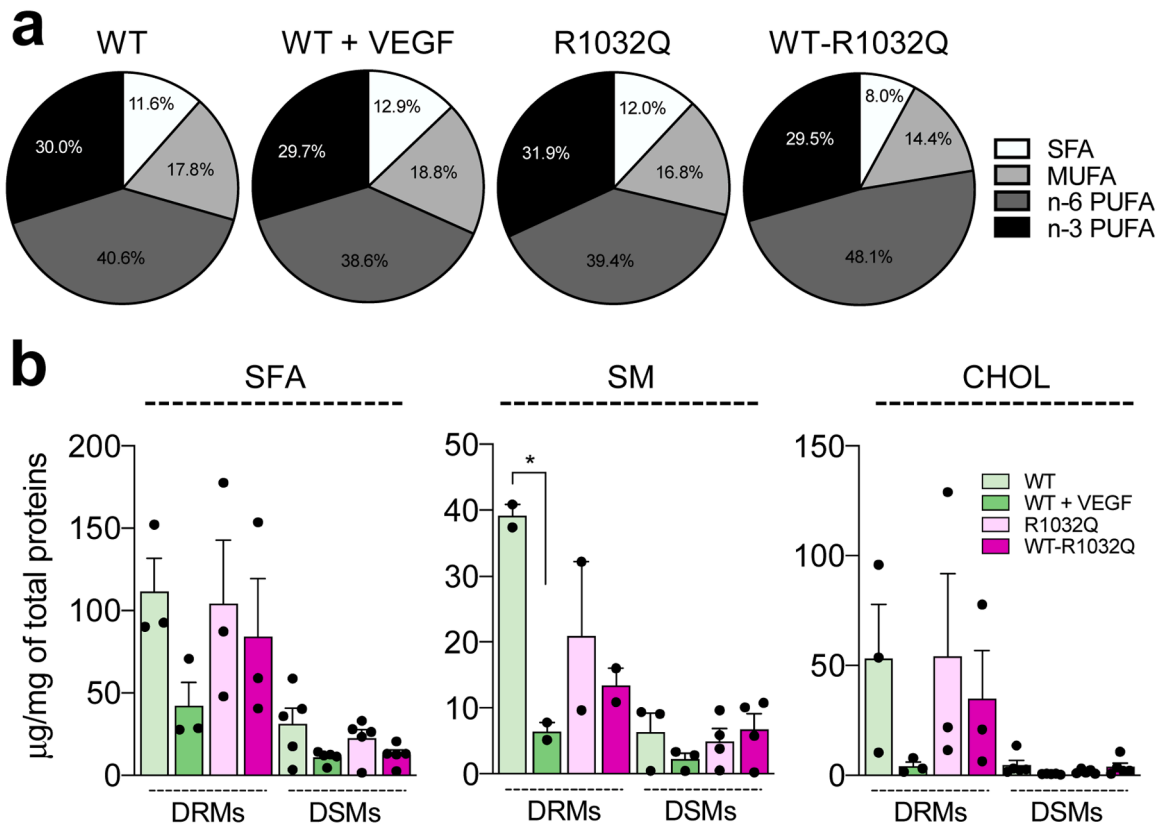

Fig. 6. Effect of VEGFR2^{WT}-VEGFR2^{R1032Q} co-expression on the lipid profile of CHO cells. **a**, analysis of total lipid content (SFAs, MUFAs and PUFAs) of CHO cells expressing VEGFR2^{WT}, VEGFR2^{R1032Q} or the couple VEGFR^{WT}-VEGFR2^{R1032Q} treated with 30 ng/mL of VEGF or left untreated. **b**, analysis of SFA, SM and cholesterol in DRM *vs* DSM fractions of CHO cells expressing VEGFR2^{WT}, VEGFR2^{R1032Q} or the couple VEGFR^{WT}-VEGFR2^{R1032Q} treated with 30 ng/mL of VEGF or left untreated. *, $p < 0.05$; **, $p < 0.01$, One-Way ANOVA followed by Dunnett's post-hoc test.

domains [24]. Thus, it is not surprising that the substitution of this arginine residue hampers the enzymatic activity abolishing the auto-phosphorylation as showed by Kumar et al. [10] and corroborated in our study.

The ability of kinases lacking auto-phosphotransferase activity, either naturally or through mutational events, to activate intracellular signaling and promote tumor progression has been described for different enzymes. The human epidermal growth factor receptor 3 (HER3) and the BRAF (D594A) mutant are prototypical examples of inactive kinases promoting breast cancer, lung adenocarcinoma, and melanoma development [25–29]. These effects can occur through different mechanisms which include forced or favored dimerization, increased affinity for adaptors and second messengers, and conformational changes [30–33]. VEGFR2^{R1032Q} fits in such a paradigm. Indeed, intrinsically inactive VEGFR2^{R1032Q} has a pro-oncogenic effect *in vitro* and *in vivo* which is mediated by its ability to dimerize with co-expressed wild-type VEGFR2. This results in the acquisition of a significant kinase activity, and receptor phosphorylation that is detectable also in tumor xenografts derived from melanoma cells co-expressing VEGFR2^{R1032Q} and endogenous VEGFR2^{WT}. Similarly, Toledo et al. [5] demonstrated that the VEGFR2^{R1032Q} expression boosts the tumorigenic capacity of the VEGFR2-expressing colo-320 cancer cell line [34]. Of note, different from the kinase-defective EGFR^{K721M} [35], VEGFR2^{R1032Q} is phosphorylated upon heterodimerization, reflecting the diversity of the mechanisms by which intrinsically inactive RTKs can act.

Our results also highlight that the co-expression of VEGFR2^{WT} and VEGFR2^{R1032Q} is sufficient to activate VEGFR2, even in the absence of ligand binding. One possible explanation is that the VEGFR2^{R1032Q} /VEGFR2^{WT} interaction induces conformational changes that activate and trans-phosphorylate both receptors. On these bases, we speculate that VEGFR2^{WT}-VEGFR2^{R1032Q} dimerization may occur in cancer patients with heterozygous VEGFR2, promoting tumor progression. In this context, the presence of VEGFR2^{R1032Q} in a given tumor could acquire prognostic significance.

Mutations in the kinase domain of RTKs often affect receptor function beyond its catalytic activity. Changes in the aminoacidic sequence and structure of the KD of VEGFR2 could alter its interactions with binding partners, leading to the modification and/or loss/acquisition of (new) functional features. For example, the R1032Q substitution could impact on VEGFR2 interaction with the CD147/emmprin receptor, which potentiates VEGFR2 activation in melanoma cells [36] or with neuropilin-2, which modulates VEGFR2-mediated intracellular signaling and drives the growth of neuroendocrine prostate cancer [37]. Our observations showed how the R1032Q mutation affects the VEGFR2 interactome (i.e. Shp2, Nck, Grb2) and modifies the phosphorylation of other membrane RTKs. Noticeably, adaptor proteins (e.g. Grb2) can modulate the lipid raft recruitment, clustering and activation of RTKs (FGFR2, EGFR, etc.) [15,16]. Thus, the impact of the R1032Q mutation on downstream effector recruitment could also explain the biological effects of VEGFR2^{R1032Q} observed in the present study. In particular, the decrease in the recruitment of the adaptor proteins Grb2 and Nck detected in cells co-expressing VEGFR2^{R1032Q} and VEGFR2^{WT} could explain the decrease in the immobile fraction of VEGFR2 as measured by FRAP analysis. This interpretation is consistent with the increase in the association of VEGFR2 with DRMs and suggests possible mechanisms driving the clustering of VEGFR2 into specific membrane regions, leading to its activation. Although these findings needs further verification, we can conclude that this mechanism could underlie, together with dimerization and trans-phosphorylation, the pro-tumorigenic role of VEGFR2^{R1032Q}.

Moreover, KD mutations can affect the response to TKi. In particular the R1032Q mutation increases receptor sensitivity to the TKi

cabozantinib and lenvatinib [7]. It remains to be defined how VEGFR2^{R1032Q}/VEGFR2^{WT} heterodimers respond to the different classes of TKi, in order to determine and predict how the presence of the R1032Q mutation in a given cancer patient could affect the response to VEGFR2-targeted TKi. We can anticipate that the presence of the mutation might increase the sensitivity to VEGFR2-targeted TKi, as shown in a case report where a good clinical response to pazopanib treatment of a patient with an advanced-stage of cutaneous cancer was demonstrated [8].

Changes in the KD can also impact receptor interaction with membrane lipids, and membrane dynamics. Membrane lipids regulate RTK activation through direct interaction with the protein structure and by modulating biophysical proprieties, e.g. changes in fluidity, hydration and thickness, providing regulatory checkpoints for receptor function. Both specific and non-specific lipid-protein interaction are crucial for RTK signaling and are proposed to underlie oncogenic constitutive activation of mutated RTKs in cancer [38,39].

During VEGFR2 activation, the transmembrane domain (TMD) exposes the amino acids E764, T771 and F778 to plasma membrane lipid interaction thus promoting an increase in KD phosphorylation [17], and making the TMD essential for stabilizing the active conformation of VEGFR2 KD. VEGFR2 co-localizes with cholesterol-rich membrane microdomains such as lipid rafts and caveolae [40] where it functionally interacts with raftlin [41], a protein necessary for lipid raft integrity. Lipid rafts facilitate VEGFR2 dimerization [23] and, as a consequence, lipid-raft disruption impairs VEGFR2 activity. However, upon activation, VEGFR2 is released from lipid rafts/caveolae to facilitate receptor internalization or translocation into focal adhesion contacts [42]. These data show how membrane lipid environment regulate VEGFR2 activity and function. The R1032Q substitution in VEGFR2, when in the presence of VEGFR2^{WT} drives the unphosphorylated total receptor towards lipid rafts. This is in line with the decreased association with Grb2, whose reduced expression was shown to facilitate FGFR2 dispersion into DRMs [16]. Also, it suggests that VEGFR2^{R1032Q} stabilizes the receptor in these domains and may reduce receptor activity. However, we demonstrated that co-expression of the two variants results in strong receptor phosphorylation with significant amounts of phosphorylated VEGFR2 localized in EEA1-positive membrane fractions. This behavior suggests that the interaction with lipid-rafts play a central role in VEGFR2 activation and oncogenic signaling, and reminds that of Kit receptor [43]. Our results support the hypothesis that receptor heterodimerization and trans-phosphorylation is one driver of these effects. However, we cannot rule out a possible contribution of VEGFR2^{R1032}-dependent receptor clustering in DRM domains, which is known to induce ligand-independent RTK activation [11]. Further studies are necessary for a precise characterization of the membrane dynamics of VEGFR2 and of lipid rafts (using single molecule tracking and Lyn-based sensors) in the presence of the mutant receptor.

Additionally, RTKs can, in turn, influence the local lipid bilayer environment by clustering raft-specific lipids such as gangliosides and by regulating lipid metabolism, which control membrane fluidity and microdomain formation [44]. These effects on membrane lipid composition rapidly follow the activation of RTK downstream signaling [45]. Changes in RTK-associated intracellular proteins can also modify the lipid composition and chemical-physical properties of membrane microdomains [16]. Here we show that the co-expression of VEGFR2^{R1032Q} with the wild-type counterpart alters the lipid raft composition, with a general decrease in raft-associated lipid (i.e. SFA, SM and cholesterol) similar to the effects of VEGF stimulation. This suggest that this lipid-raft dismantling, that could be mediated by enzymes (e.g. acid sphingomyelinase) activated downstream to VEGFR2 activation [45], may sustain ligand-independent VEGFR2 activation and possibly other RTKs in order to promote oncogenic signaling and cancer progression. Future studies will deepen how the R1032Q mutations affect the interactions between VEGFR2 and membrane lipids to evaluate the opportunity of novel targets to block the oncogenic activation of VEGFR2.

The study of the pro-oncogenic mechanism of VEGFR2^{R1032Q} acquires greater translational importance when considering that the substitution of the arginine at this given position within the KD recurs in multiple kinases, including ERBB2, CHEK2, TGFBR1, FLT3, BRAF, FLT1, FGFR4, FLT4 and TIE1[10,46]. Based on previous studies [46–48], we speculate that mutations clustering at this position could affect the kinases with a mechanism (inactivating and heterodimerization-dependent) similar to the R1032Q mutation of VEGFR2. This is confirmed by scattered studies showing that these mutations exhibit superimposable effects on enzyme activity, all entailing kinase inactivation [49–51].

In conclusion, we have characterized a novel oncogenic activation mechanism for VEGFR2 which could apply also to corresponding uncharacterized cancer-associated mutants. This mechanism could represent in the future a molecular target to halt the progression of those tumors harboring these inactivating mutations of RTKs.

Ethics Approval

In vivo experiments, approved by Italian "Ministero della Salute" (authorization 266/2016-PR), were performed in accordance with national and European guidelines and regulations for laboratory animal use in research.

Availability of data and materials

All data needed to evaluate conclusions in the paper are present either in the figures or in the text. Additional information as well as plasmids and cell lines generated in this study are available upon request to the lead contact, Stefania Mitola: stefania.mitola@unibs.it.

Declaration of generative AI in scientific writing

We declare that no AI-assisted technologies were applied in the writing process of this manuscript.

CRediT authorship contribution statement

Cosetta Ravelli: Writing – review & editing, Writing – original draft, Methodology, Investigation, Formal analysis, Data curation, Conceptualization. **Michela Corsini:** Writing – review & editing, Methodology, Investigation, Formal analysis, Data curation. **Roberto Bresciani:** Writing – review & editing, Formal analysis, Data curation. **Angela M. Rizzo:** Writing – review & editing, Formal analysis, Data curation. **Luca Zammataro:** Writing – review & editing, Formal analysis, Data curation. **Paola A. Corsetto:** Writing – review & editing, Methodology, Investigation, Formal analysis, Data curation. **Elisabetta Grillo:** Writing – review & editing, Writing – original draft, Project administration, Methodology, Investigation, Formal analysis, Data curation, Conceptualization. **Stefania Mitola:** Writing – review & editing, Writing – original draft, Project administration, Methodology, Investigation, Funding acquisition, Formal analysis, Data curation, Conceptualization.

Declaration of competing interest

The authors declare that they have no known competing financial interests or personal relationships that could have appeared to influence the work reported in this paper.

Acknowledgements

The authors are grateful to Prof. Marco Presta (University of Brescia, Italy) for helpful discussion; to Prof. Kurt Ballmer-Hofer (Paul Scherrer Institute, Villigen, Switzerland) for discussion and for having provided plasmids; to Dr. Kalina Hristova (Johns Hopkins University, Baltimore, Maryland, USA) for having provided plasmids. The authors performed

experiments at the Animal house and at the Imaging Platform of the Department of Translational and Molecular Medicine of the University of Brescia.

Funding

This work was supported by grants from MIUR to Consorzio Interuniversitario Biotecnologie (CIB), from Associazione Italiana Ricerca sul Cancro to S.M. (AIRC grant IG17276) and from University of Brescia (Fondi Locali per la Ricerca) to R.B., E.G., M.C. and S.M. M.C. was supported by AIRC fellowship for Italy (grant n° 26917). S.M. and M.C. were supported by "PNRR M4C2-Investimento 1.4-CN00000041 finanziato dall'Unione Europea–NextGenerationEU"). E.G was supported by Fondazione Umberto Veronesi Fellowships. Funding bodies did not have any role in designing the study, collecting, analyzing, and interpreting data or in writing the manuscript.

Supplementary materials

Supplementary material associated with this article can be found, in the online version, at doi:10.1016/j.neo.2025.101195.

References

[1] A.M. Devery, R. Wadekar, S.M. Bokobza, A.M. Weber, Y. Jiang, A.J. Ryan, Vascular endothelial growth factor directly stimulates tumour cell proliferation in non-small cell lung cancer, Int. J. Oncol. 47 (2015) 849–856, https://doi.org/10.3892/ijo.2015.3082.

[2] L. Lian, X.L. Li, M.D. Xu, X.M. Li, M.Y. Wu, Y. Zhang, M. Tao, W. Li, X.M. Shen, C. Zhou, et al., VEGFR2 promotes tumorigenesis and metastasis in a pro-angiogenic-independent way in gastric cancer, BMC Cancer 19 (2019) 183, https://doi.org/10.1186/s12885-019-5322-0.

[3] J. Graells, A. Vinyals, A. Figueras, A. Llorens, A. Moreno, J. Marcoval, F. J. Gonzalez, A. Fabra, Overproduction of VEGF concomitantly expressed with its receptors promotes growth and survival of melanoma cells through MAPK and PI3K signaling, J. Invest. Dermatol. 123 (2004) 1151–1161, https://doi.org/10.1111/j.0022-202X.2004.23460.x.

[4] I.P. Silva, A. Salhi, K.M. Giles, M. Vogelsang, S.W. Han, N. Ismaili, K.P. Lui, E. M. Robinson, M.A. Wilson, R.L. Shapiro, et al., Identification of a novel pathogenic germline KDR variant in Melanoma, Clin. Cancer Res. 22 (2016) 2377–2385, https://doi.org/10.1158/1078-0432.CCR-15-1811.

[5] R.A. Toledo, E. Garralda, M. Mitsi, T. Pons, J. Monsech, E. Vega, A. Otero, M. I. Albarran, N. Banos, Y. Duran, et al., Exome sequencing of plasma DNA portrays the mutation landscape of colorectal cancer and discovers mutated VEGFR2 receptors as modulators of antiangiogenic therapies, Clin. Cancer Res. 24 (2018) 3550–3559, https://doi.org/10.1158/1078-0432.CCR-18-0103.

[6] E. Grillo, M. Corsini, C. Ravelli, M. di Somma, L. Zammataro, E. Monti, M. Presta, S. Mitola, A novel variant of VEGFR2 identified by a pan-cancer screening of recurrent somatic mutations in the catalytic domain of tyrosine kinase receptors enhances tumor growth and metastasis, Cancer Lett. 496 (2020) 84–92, https://doi.org/10.1016/j.canlet.2020.09.027.

[7] A. Loaiza-Bonilla, C.E. Jensen, S. Shroff, E. Furth, P.A. Bonilla-Reyes, A.F. Deik, J. Morrissette, KDR mutation as a novel predictive biomarker of exceptional response to Regorafenib in metastatic colorectal cancer, Cureus 8 (2016) e478, https://doi.org/10.7759/cureus.478.

[8] T.C. Knepper, M.L. Freeman, G.T. Gibney, H.L. McLeod, J.S. Russell, Clinical response to Pazopanib in a patient with KDR-mutated metastatic basal cell carcinoma, JAMA Dermatol 153 (2017) 607–609, https://doi.org/10.1001/jamadermatol.2017.0187.

[9] Y. Cui, P. Zhang, X. Liang, J. Xu, X. Liu, Y. Wu, J. Zhang, W. Wang, F. Zhang, R. Guo, Association of KDR mutation with better clinical outcomes in pan-cancer for immune checkpoint inhibitors, Am J Cancer Res 12 (2022) 1766–1783.

[10] R.D. Kumar, R. Bose, Analysis of somatic mutations across the kinome reveals loss-of-function mutations in multiple cancer types, Sci. Rep. 7 (2017) 6418, https://doi.org/10.1038/s41598-017-06366-x.

[11] J.B. Casaletto, A.I. McClatchey, Spatial regulation of receptor tyrosine kinases in development and cancer, Nat. Rev. Cancer 12 (2012) 387–400, https://doi.org/10.1038/nrc3277.

[12] S. Tsukamoto, Y. Huang, M. Kumazoe, C. Lesnick, S. Yamada, N. Ueda, T. Suzuki, S. Yamashita, Y.H. Kim, Y. Fujimura, et al., Sphingosine kinase-1 protects multiple myeloma from apoptosis driven by cancer-specific inhibition of RTKs, Mol. Cancer Ther. 14 (2015) 2303–2312, https://doi.org/10.1158/1535-7163.MCT-15-0185.

[13] E. Wahlen, F. Olsson, D. Raykova, O. Soderberg, J. Heldin, J. Lennartsson, Activated EGFR and PDGFR internalize in separate vesicles and downstream AKT and ERK1/2 signaling are differentially impacted by cholesterol depletion, Biochem. Biophys. Res. Commun. 665 (2023) 195–201, https://doi.org/10.1016/j.bbrc.2023.04.099.

[14] S.T. Low-Nam, K.A. Lidke, P.J. Cutler, R.C. Roovers, P.M. van Bergen en Henegouwen, B.S. Wilson, D.S. Lidke, ErbB1 dimerization is promoted by domain co-confinement and stabilized by ligand binding, Nat. Struct. Mol. Biol. 18 (2011) 1244–1249, https://doi.org/10.1038/nsmb.2135.

[15] C.Y. Lin, J.Y. Huang, L.W. Lo, Unraveling the impact of lipid domains on the dimerization processes of single-molecule EGFRs of live cells, Biochim. Biophys. Acta 1848 (2015) 886–893, https://doi.org/10.1016/j.bbamem.2014.12.019.

[16] A. Rohwedder, S. Knipp, L.D. Roberts, J.E. Ladbury, Composition of receptor tyrosine kinase-mediated lipid micro-domains controlled by adaptor protein interaction, Sci. Rep. 11 (2021) 6160, https://doi.org/10.1038/s41598-021-85578-8.

[17] S. Sarabipour, K. Ballmer-Hofer, K. Hristova, VEGFR-2 conformational switch in response to ligand binding, eLife 5 (2016) e13876, https://doi.org/10.7554/eLife.13876.

[18] G. Baldanzi, S. Mitola, S. Cutrupi, N. Filigheddu, W.J. van Blitterswijk, F. Sinigaglia, F. Bussolino, A. Graziani, Activation of diacylglycerol kinase alpha is required for VEGF-induced angiogenic signaling in vitro, Oncogene 23 (2004) 4828–4838, https://doi.org/10.1038/sj.onc.1207633.

[19] M.A. Rizzo, G. Springer, K. Segawa, W.R. Zipfel, D.W. Piston, Optimization of pairings and detection conditions for measurement of FRET between cyan and yellow fluorescent proteins, Microsc. Microanal. 12 (2006) 238–254, https://doi.org/10.1017/S1431927606060235.

[20] M. Corsini, C. Ravelli, E. Grillo, M. Domenichini, S. Mitola, Mutation in the Kinase domain alters the VEGFR2 membrane dynamics, Cells 13 (2024), https://doi.org/10.3390/cells13161346.

[21] E.A. Reits, J.J. Neefjes, From fixed to FRAP: measuring protein mobility and activity in living cells, Nat. Cell Biol. 3 (2001) E145–E147, https://doi.org/10.1038/35078615.

[22] P. Mereghetti, P.A. Corsetto, A. Cremona, A.M. Rizzo, S.M. Doglia, D. Ami, A fourier transform infrared spectroscopy study of cell membrane domain modifications induced by docosahexaenoic acid, Biochim. Biophys. Acta 1840 (2014) 3115–3122, https://doi.org/10.1016/j.bbagen.2014.07.003.

[23] M. Simons, E. Gordon, L. Claesson-Welsh, Mechanisms and regulation of endothelial VEGF receptor signalling, Nat. Rev. Mol. Cell Biol. 17 (2016) 611–625, https://doi.org/10.1038/nrm.2016.87.

[24] R. Kalaivani, T.J. Narwani, A.G. de Brevern, N. Srinivasan, Long-range molecular dynamics show that inactive forms of Protein Kinase A are more dynamic than active forms, Protein Sci. 28 (2019) 543–560, https://doi.org/10.1002/pro.3556.

[25] A.S. Berghoff, R. Bartsch, M. Preusser, G. Ricken, G.G. Steger, Z. Bago-Horvath, M. Rudas, B. Streubel, P. Dubsky, M. Gnant, et al., Co-overexpression of HER2/HER3 is a predictor of impaired survival in breast cancer patients, Breast 23 (2014) 637–643, https://doi.org/10.1016/j.breast.2014.06.011.

[26] S.J. Heidorn, C. Milagre, S. Whittaker, A. Nourry, I. Niculescu-Duvas, N. Dhomen, J. Hussain, J.S. Reis-Filho, C.J. Springer, C. Pritchard, et al., Kinase-dead BRAF and oncogenic RAS cooperate to drive tumor progression through CRAF, Cell 140 (2010) 209–221, https://doi.org/10.1016/j.cell.2009.12.040.

[27] N.J. Cope, B. Novak, Z. Liu, M. Cavallo, A.Y. Gunderwala, M. Connolly, Z. Wang, Analyses of the oncogenic BRAF(D594G) variant reveal a kinase-independent function of BRAF in activating MAPK signaling, J. Biol. Chem. 295 (2020) 2407–2420, https://doi.org/10.1074/jbc.RA119.011536.

[28] M.T. Chang, S. Asthana, S.P. Gao, B.H. Lee, J.S. Chapman, C. Kandoth, J. Gao, N. D. Socci, D.B. Solit, A.B. Olshen, et al., Identifying recurrent mutations in cancer reveals widespread lineage diversity and mutational specificity, Nat. Biotechnol. 34 (2016) 155–163, https://doi.org/10.1038/nbt.3391.

[29] P. Nieto, C. Ambrogio, L. Esteban-Burgos, G. Gomez-Lopez, M.T. Blasco, Z. Yao, R. Marais, N. Rosen, R. Chiarle, D.G. Pisano, et al., A Braf kinase-inactive mutant induces lung adenocarcinoma, Nature 548 (2017) 239–243, https://doi.org/10.1038/nature23297.

[30] J.A. Menendez, R. Lupu, Transphosphorylation of kinase-dead HER3 and breast cancer progression: a new standpoint or an old concept revisited? Breast Cancer Res. 9 (2007) 111, https://doi.org/10.1186/bcr1773.

[31] L. Gao, Y. Zhang, M. Feng, M. Shen, L. Yang, B. Wei, Y. Zhou, Z. Zhang, HER3: updates and current biology function, targeted therapy and pathologic detecting methods, Life Sci. 357 (2024) 123087, https://doi.org/10.1016/j.lfs.2024.123087.

[32] V. Nawaratne, A.K. Sondhi, O. Abdel-Wahab, J. Taylor, New means and challenges in the targeting of BTK, Clin. Cancer Res. 30 (2024) 2333–2341, https://doi.org/10.1158/1078-0432.CCR-23-0409.

[33] R. Thomas, S. Srivastava, R.R. Katreddy, J. Sobieski, Z. Weihua, Kinase-inactivated EGFR is required for the survival of wild-type EGFR-expressing cancer cells treated with tyrosine Kinase inhibitors, Int. J. Mol. Sci. 20 (2019), https://doi.org/10.3390/ijms20102515.

[34] K.B. Tran, S. Kolekar, Q. Wang, J.H. Shih, C.M. Buchanan, S. Deva, P.R. Shepherd, Response to BRAF-targeted therapy is enhanced by Cotargeting VEGFRs or WNT/beta-catenin signaling in BRAF-mutant colorectal cancer models, Mol. Cancer Ther. 21 (2022) 1777–1787, https://doi.org/10.1158/1535-7163.MCT-21-0941.

[35] J. Rauch, N. Volinsky, D. Romano, W. Kolch, The secret life of kinases: functions beyond catalysis, Cell Commun. Signal. 9 (2011) 23, https://doi.org/10.1186/1478-811X-9-23.

[36] F. Khayati, L. Perez-Cano, K. Maouche, A. Sadoux, Z. Boutalbi, M.P. Podgorniak, U. Maskos, N. Setterblad, A. Janin, F. Calvo, et al., EMMPRIN/CD147 is a novel coreceptor of VEGFR-2 mediating its activation by VEGF, Oncotarget 6 (2015) 9766–9780, https://doi.org/10.18632/oncotarget.2870.

[37] J. Wang, J. Li, L. Yin, T. Pu, J. Wei, V. Karthikeyan, T.P. Lin, A.C. Gao, B.J. Wu, Neuropilin-2 promotes lineage plasticity and progression to neuroendocrine prostate cancer, Oncogene 41 (2022) 4307–4317, https://doi.org/10.1038/s41388-022-02437-0.

[38] E.V. Bocharov, G.V. Sharonov, O.V. Bocharova, K.V. Pavlov, Conformational transitions and interactions underlying the function of membrane embedded

receptor protein kinases, Biochim. Biophys Acta. Biomembr 1859 (2017) 1417–1429, https://doi.org/10.1016/j.bbamem.2017.01.025.
[39] G. Hedger, M.S. Sansom, H. Koldso, The juxtamembrane regions of human receptor tyrosine kinases exhibit conserved interaction sites with anionic lipids, Sci. Rep. 5 (2015) 9198, https://doi.org/10.1038/srep09198.
[40] L. Labrecque, I. Royal, D.S. Surprenant, C. Patterson, D. Gingras, R. Beliveau, Regulation of vascular endothelial growth factor receptor-2 activity by caveolin-1 and plasma membrane cholesterol, Mol. Biol. Cell 14 (2003) 334–347, https://doi.org/10.1091/mbc.e02-07-0379.
[41] A.L. Bayliss, A. Sundararaman, C. Granet, H. Mellor, Raftlin is recruited by neuropilin-1 to the activated VEGFR2 complex to control proangiogenic signaling, Angiogenesis 23 (2020) 371–383, https://doi.org/10.1007/s10456-020-09715-z.
[42] S. Ikeda, M. Ushio-Fukai, L. Zuo, T. Tojo, S. Dikalov, N.A. Patrushev, R. W. Alexander, Novel role of ARF6 in vascular endothelial growth factor-induced signaling and angiogenesis, Circ. Res. 96 (2005) 467–475, https://doi.org/10.1161/01.RES.0000158286.51045.16.
[43] T. Jahn, E. Leifheit, S. Gooch, S. Sindhu, K. Weinberg, Lipid rafts are required for Kit survival and proliferation signals, Blood 110 (2007) 1739–1747, https://doi.org/10.1182/blood-2006-05-020925.
[44] J. Zhang, F. Song, X. Zhao, H. Jiang, X. Wu, B. Wang, M. Zhou, M. Tian, B. Shi, H. Wang, et al., EGFR modulates monounsaturated fatty acid synthesis through phosphorylation of SCD1 in lung cancer, Mol. Cancer 16 (2017) 127, https://doi.org/10.1186/s12943-017-0704-x.
[45] Y.H. Zeidan, Y.A. Hannun, Activation of acid sphingomyelinase by protein kinase cdelta-mediated phosphorylation, J. Biol. Chem. 282 (2007) 11549–11561, https://doi.org/10.1074/jbc.M609424200.
[46] E. Grillo, C. Ravelli, M. Corsini, C. Gaudenzi, L. Zammataro, S. Mitola, Novel potential oncogenic and druggable mutations of FGFRs recur in the kinase domain across cancer types, Biochim. Biophys. Acta. Mol. Basis Dis. (2021) 166313, https://doi.org/10.1016/j.bbadis.2021.166313.
[47] M.L. Miller, E. Reznik, N.P. Gauthier, B.A. Aksoy, A. Korkut, J. Gao, G. Ciriello, N. Schultz, C. Sander, Pan-cancer analysis of mutation hotspots in protein domains, Cell Syst. 1 (2015) 197–209, https://doi.org/10.1016/j.cels.2015.08.014.
[48] E. Grillo, C. Ravelli, M. Corsini, L. Zammataro, S. Mitola, Protein domain-based approaches for the identification and prioritization of therapeutically actionable cancer variants, Biochim. Biophys. Acta. Rev. Cancer. (2021) 188614, https://doi.org/10.1016/j.bbcan.2021.188614.
[49] O. Tetsu, J. Phuchareon, A. Chou, D.P. Cox, D.W. Eisele, R.C. Jordan, Mutations in the c-Kit gene disrupt mitogen-activated protein kinase signaling during tumor development in adenoid cystic carcinoma of the salivary glands, Neoplasia 12 (2010) 708–717, https://doi.org/10.1593/neo.10356.
[50] C.Q. Cai, Y. Peng, M.T. Buckley, J. Wei, F. Chen, L. Liebes, W.L. Gerald, M. R. Pincus, I. Osman, P. Lee, Epidermal growth factor receptor activation in prostate cancer by three novel missense mutations, Oncogene 27 (2008) 3201–3210, https://doi.org/10.1038/sj.onc.1210983.
[51] A.L. Evans, R. Bell, G. Brice, P. Comeglio, C. Lipede, S. Jeffery, P. Mortimer, M. Sarfarazi, A.H. Child, Identification of eight novel VEGFR-3 mutations in families with primary congenital lymphoedema, J. Med. Genet. 40 (2003) 697–703, https://doi.org/10.1136/jmg.40.9.697.